ELSEVIER

Agricultural and Forest Meteorology 105 (2000) 21–41

AGRICULTURAL AND FOREST METEOROLOGY

www.elsevier.com/locate/agrformet

PAR extinction in shortgrass ecosystems: effects of clumping, sky conditions and soil albedo

Yann Nouvellon [a,*], Agnès Bégué [b], M. Susan Moran [a], Danny Lo Seen [b], Serge Rambal [c], Delphine Luquet [b], Ghani Chehbouni [d], Yoshio Inoue [e]

[a] *USDA–ARS–SWRC, SW Watershed Research Center, 2000 E. Allen Road, Tucson, AZ 85719, USA*
[b] *CIRAD–AMIS, Maison de la Télédétection, Montpellier, France*
[c] *CEFE–CNRS, DREAM Unit, Montpellier, France*
[d] *ORSTOM/IMADES, Hermosillo, Mexico*
[e] *National Institute of Agro-environmental Sciences, Tsukuba, Ibaraki, Japan*

Abstract

The amount of photosynthetically active radiation (PAR) absorbed by a canopy (APAR) is an important driving variable for vegetation processes such as photosynthesis. PAR extinction in clumped canopies of shortgrass ecosystems is the focus of this paper. Directional gap fractions estimated at peak biomass on several Mexican shortgrass ecosystems with a hemispherical radiation sensor (Li-Cor, LAI-2000) were higher than those predicted by a Poisson model assuming a random leaf dispersion (RLD). LAI-2000-estimated gap fractions, together with independent estimations of plant area index (PAI), and leaf and stem angle distribution (LSAD) were used for estimating the angular course of a leaf dispersion parameter $\lambda(\theta)$. Radiation extinction coefficients simulated for all solar zenith angles using Markov chain processes and estimated $\lambda(\theta)$ were subsequently incorporated in a simple radiative transfer model for estimating the efficiencies of instantaneous and daily integrated PAR interception and absorption, and for studying the effects of clumping, sky conditions and soil albedo on PAR absorption. For clear sky condition, instantaneous PAR absorption showed marked directional effects, therefore indicating that using a constant extinction coefficient in canopy photosynthesis models working at hourly time step would be inaccurate. The effects of clumping, sky conditions and soil albedo were all found to be significant for low PAI, and decreased with higher PAI. As shortgrass ecosystems are characterized by low PAI, neglecting these effects would give inaccurate estimations of PAR absorption.

Daily PAR absorption was found to be significantly higher than PAR interception for low PAI, especially when soil albedo was high, and lower than PAR interception for high PAI. These results indicate that in canopy photosynthesis models where APAR is estimated from simple exponential-like relationships calibrated using PAR interception measurements, the PAR available for photosynthesis might be significantly underestimated in the first stages of the growth, and may be overestimated in the later stages of the growing season.

Keywords: PAR interception; PAR absorption; Extinction coefficient; Markov model; Shortgrass ecosystem

1. Introduction

The instantaneous or daily integrated photosynthetically active radiation (PAR) absorbed by a canopy (APAR) is an important input for canopy photosynthesis models working either at an instantaneous or

* Corresponding author. Tel.: +1-520-670-6380; fax: +1-520-670-5550.
E-mail address: yann@tucson.ars.ag.gov (Y. Nouvellon).

0168-1923/00/$ – see front matter
PII: S0168-1923(00)00194-5

daily timescale. While APAR or its related fractional efficiency (f_{APAR}) is the most relevant quantity to describe the energy flux available for photosynthesis, this latter is often estimated from a less relevant but more easily estimable quantity, the intercepted PAR (IPAR) (or its related fractional efficiency, f_{IPAR}), simply expressed as the difference between incoming PAR and the PAR transmitted to the soil through the canopy. f_{IPAR} depends on the foliage amount, canopy structure (leaf dispersion and leaf angle distribution), leaf optical properties, solar angle and the proportion of diffuse radiation, while f_{APAR} is also dependent on soil optical properties (soil reflectance). Although IPAR is often used to estimate the available radiation for photosynthesis, it is generally reported to be significantly higher than APAR for closed canopies (e.g. Le Roux et al., 1997), and may be lower than APAR for poorly developed clumped canopies with high soil albedo (Bégué et al., 1996a).

APAR or IPAR can be estimated by radiative transfer models assuming a homogeneous canopy (e.g. SAIL model, Verhoef, 1984), or based on a detailed description of the canopy structure (e.g. DART model, Gastellu-Etchegorry et al., 1996). Turbid medium models may be inaccurate for clumped canopies (e.g. Bégué et al., 1996b; Luquet et al., 1998), and 3D radiative transfer models are difficult to parameterize and/or are time consuming, so that in canopy photosynthesis models IPAR or APAR are often computed with much simpler models generally based on the Beer Lambert equation

$$f_{IPAR} \text{ or } f_{APAR} = 1 - \exp(-k\,\mathrm{PAI}), \quad (1)$$

where k is an extinction coefficient, for instantaneous or daily integrated PAR interception or absorption, and PAI the plant area index (the sum of leaf area index and stem area index).

This exponential relationship with PAI generally gives realistic IPAR or APAR estimations. Values of extinction coefficients for instantaneous or daily integrated interception or absorption have been reported for several crop canopies (e.g. Monteith, 1969; Hipps et al., 1983; Gallo et al., 1985; Maas, 1988; Bégué, 1991), and forage species (e.g. Sheehy and Peacock, 1975; Woledge and Parsons, 1986). However, for some major natural ecosystems such as shortgrass ecosystems which cover large parts of the land surface, these coefficients are still poorly documented. Furthermore, even when estimates of k are available, they may be dependent on the conditions for which they were obtained (proportion of diffuse radiation and soil albedo) so that their use under other soil albedos or sky conditions may be inappropriate. In order to avoid these problems, it is more relevant to describe the extinction coefficients by considering (1) direct beam and diffuse radiation interception separately (total radiation interception and absorption can be estimated by taking into account the relative proportion of diffuse and direct beam in the incoming PAR), and (2) soil albedo in the case of PAR absorption.

For homogeneous canopies, several models based on probability statistics have been used to estimate the extinction coefficients by taking into account the leaf angle distribution (LAD) or the mean tilt angle (MTA) (e.g. Warren Wilson, 1960; Saeki, 1963; Miller, 1967; Cowan, 1968; Monteith, 1969). In most cases, a random leaf dispersion (RLD) is assumed, and a Poisson model is used. However, this assumption does not hold for canopies with clumped leaf dispersions, which are known to have lower extinction coefficients than those with randomly dispersed leaves (e.g. Nilson, 1971; Lemeur and Blad, 1974; Baldocchi and Collineau, 1994). For such canopies, models based on negative binomial probability functions or on the theory of Markov processes have been proposed (Nilson, 1971). These models introduce a clumping factor that is unknown and must be determined. Due to the difficulty in mechanistically determining the clumping factor, empirical estimation is a useful alternative (Lemeur and Blad, 1974; Ross, 1975; Baldocchi and Collineau, 1994). For this purpose, directional interception measurements obtained with a commercially available hemispherical radiation sensor (Li-Cor, LAI-2000) may be valuable.

The objective of this paper is to document the PAR extinction coefficients in shortgrass ecosystems in northwestern Mexico. Directional interceptions measured by an LAI-2000 and simultaneous independent measurements of PAI are first used to estimate the clumping factor of the Markov model, and its directional dependence. The Markov model is subsequently used for computing extinction coefficients for direct interception for all solar zenith angles. The results are then used to compute diffuse radiation interception, as well as instantaneous and daily integrated total radiation interception and absorption with

varying PAI, sky conditions and soil albedo. These allow us to estimate generalized extinction coefficients for daily interception or absorption, and to evaluate the errors expected by not taking into account the sky conditions or by assuming IPAR equals APAR.

After a brief presentation of the equations used to calculate PAR interception and absorption in homogeneous canopies (Section 2.1), the methodology adopted to estimate extinction coefficients from measurements of 'gap fraction' measured with an LAI-2000 is given (Section 2.2). The experiment and the test sites are described in Section 3; the results obtained are presented in Section 4 and discussed in Section 5.

2. Theory

2.1. Equations used to calculate PAR interception and absorption in homogeneous canopies

2.1.1. Instantaneous interception

At any time of the day, the efficiency with which incoming PAR is intercepted by a canopy depends on its efficiency to intercept direct and diffuse incoming radiation, and on the proportions of diffuse and direct radiation in the incoming PAR

$$f_{\mathrm{IPAR}}(t) = P_{\mathrm{diffuse}}(t)\, f_{\mathrm{diffuse}}(t) + P_{\mathrm{direct}}(t)\, f_{\mathrm{direct}}(t), \tag{2}$$

where $P_{\mathrm{diffuse}}(t)$, $P_{\mathrm{direct}}(t)$, and $f_{\mathrm{diffuse}}(t)$, $f_{\mathrm{direct}}(t)$ represent the proportions of the diffuse and direct radiation, and the interception efficiencies of diffuse and direct radiation at instant t, respectively.

At the solar zenith angle θ corresponding to time t, the transmission of direct radiation through the canopy, $T(\theta)$ ($T(\theta)$ being the complement of $f_{\mathrm{direct}}(\theta)$) depends on the canopy structure, foliage amount, and leaf optical properties.

In the case of a homogeneous and infinite canopy, where leaves are supposed to be randomly dispersed and black (transmittance=0), the transmission $T(\theta)$ or 'gap fraction' can be expressed as (e.g. Warren Wilson, 1963, 1965; Anderson, 1966)

$$T(\theta) = \exp\left[\frac{-G(\theta)}{\cos\theta}\mathrm{PAI}\right], \tag{3}$$

where the ratio $G(\theta)/\cos\theta$ is the directional extinction coefficient ($k(\theta)$) of direct radiation in the canopy, and $G(\theta)$ the fraction of foliage projected in the direction θ, given by

$$G(\theta_{\mathrm{s}}) = \int_0^{\pi/2} A(\theta_{\mathrm{s}}, \theta_{\mathrm{l}}) g(\theta_{\mathrm{l}})\, \mathrm{d}\theta_{\mathrm{l}}, \tag{4}$$

where $g(\theta_{\mathrm{l}})$ is the leaf inclination angle distribution function (De Wit, 1965; Goel and Strebel, 1984; Campbell, 1986, 1990), and $A(\theta_{\mathrm{s}}, \theta_{\mathrm{l}})$ the projection of unit leaf area with an inclination angle θ_{l}. $A(\theta_{\mathrm{s}}, \theta_{\mathrm{l}})$ is given by Warren Wilson (1960) as

$$\begin{aligned} &A(\theta_{\mathrm{s}}, \theta_{\mathrm{l}}) = \cos(\theta_{\mathrm{s}})\cos(\theta_{\mathrm{l}}) \qquad \text{if } \theta_{\mathrm{s}} + \theta_{\mathrm{l}} \le \frac{\pi}{2}, \\ &A(\theta_{\mathrm{s}}, \theta_{\mathrm{l}}) = \cos(\theta_{\mathrm{s}})\cos(\theta_{\mathrm{l}}) \\ &\quad \times \left|\frac{2(\Phi_0 - \tan(\Phi_0))}{\pi} - 1\right| \quad \text{if } \theta_{\mathrm{s}} + \theta_{\mathrm{l}} > \frac{\pi}{2}, \end{aligned} \tag{5}$$

with $\Phi_0 = a\cos(-\cot(\theta_{\mathrm{s}})/\tan(\theta_{\mathrm{l}}))$.

In most of the solar spectrum, since leaves cannot be considered as opaque elements, the extinction coefficient $k(\theta)$ should be multiplied by $(1-\tau_{\mathrm{f}})$, where τ_{f} is the mean leaf transmittance in the PAR region (Monteith, 1969):

$$T(\theta) = \exp[-k(\theta)(1-\tau_{\mathrm{f}})\mathrm{PAI}]. \tag{6}$$

Finally, in a homogeneous canopy, the directional direct radiation interception is expressed as

$$f_{\mathrm{direct}}(\theta) = 1 - \exp[-k(\theta)(1-\tau_{\mathrm{f}})\mathrm{PAI}]. \tag{7}$$

The computation of instantaneous total interception also requires the efficiency of diffuse radiation interception. It can be estimated following Welles and Norman (1991):

$$f_{\mathrm{diffuse}} = 1 - \frac{\int_0^{\pi/2} \Gamma(\theta) T(\theta) \sin\theta\cos\theta\, \mathrm{d}\theta}{\int_0^{\pi/2} \Gamma(\theta)\sin\theta\cos\theta\, \mathrm{d}\theta}, \tag{8}$$

where $\Gamma(\theta)$ is the intensity distribution of the diffuse radiation above the canopy.

2.1.2. Instantaneous absorption

The instantaneous absorption can be expressed as a function of the instantaneous interception, soil reflectance ρ_{s}, and vegetation optical properties (absorptance a_{l} and reflectance ρ_{l}, e.g. Bégué, 1992):

$$f_{\mathrm{APAR}}(\theta) = \frac{a_{\mathrm{l}}}{(a_{\mathrm{l}} + \rho_{\mathrm{l}})}\{f_{\mathrm{IPAR}}(\theta) + [1 - f_{\mathrm{IPAR}}(\theta)]\rho_{\mathrm{s}} f_{\mathrm{diffuse}}\}. \quad (9)$$

This expression includes the down-welling intercepted flux and an up-welling intercepted flux which comes from the reflection by the soil of the transmitted radiation towards the canopy; the up-welling flux is intercepted with an efficiency f_{diffuse}.

2.1.3. Daily integrated interception and absorption

As soon as instantaneous incoming PAR ($\mathrm{PAR}_0(t)$) is measured all over the day, and instantaneous interception and absorption are computed, daily integrated interception and absorption efficiencies can simply be expressed as

$$f_{\mathrm{DIPAR}} = \frac{\int_{t_0}^{t_n} f_{\mathrm{IPAR}}(t)\mathrm{PAR}_0(t)\,\mathrm{d}t}{\int_{t_0}^{t_n} \mathrm{PAR}_0(t)\,\mathrm{d}t},$$
$$f_{\mathrm{DAPAR}} = \frac{\int_{t_0}^{t_n} f_{\mathrm{APAR}}(t)\mathrm{PAR}_0(t)\,\mathrm{d}t}{\int_{t_0}^{t_n} \mathrm{PAR}_0(t)\,\mathrm{d}t}, \quad (10)$$

where t_0 and t_n are the times of sunrise and sunset, respectively.

It is worthwhile to point out that in the model presented above, the extinction coefficient $k(\theta)$ depends only on canopy structure. As it is involved in the computation of $T(\theta)$, and subsequently $f_{\mathrm{direct}}(\theta)$, f_{diffuse}, $f_{\mathrm{IPAR}}(\theta)$, and $f_{\mathrm{APAR}}(\theta)$, it appears to be the most critical parameter of this model and needs to be correctly estimated. However, the Poisson model used to derive Eq. (3) assumes that foliage elements are randomly dispersed. This assumption does not hold for canopies with regular leaf dispersion, where the model is known to overestimate the gap fraction, and for canopies with clumped dispersion, where gap fraction is underestimated (e.g. Nilson, 1971; Ross, 1981; Oker-Blom and Kellomaki, 1983; Baldocchi et al., 1985; Andrieu and Sinoquet, 1993; Chen et al., 1994; van Gardingen et al., 1999). Such underestimation may be significant in the highly clumped canopies of shortgrass ecosystems. For canopies with non-random leaf dispersion, Nilson (1971) has proposed a statistical model based on the theory of Markov processes. The model allows the computation of the extinction coefficient of the heterogeneous canopy by multiplying $k(\theta)$ by a coefficient λ. LAI-2000 gap fraction measurements might be useful to estimate this coefficient.

Hanan and Bégué (1995) proposed a methodology that was not based on the Markov model for computing radiation interception for all solar zenith angles using directional interception measurements performed by an LAI-2000. After a brief description of the LAI-2000 optical sensor, this methodology is presented, as well as its main drawbacks and limitations. We then describe the methodology that will be used in this study to derive the coefficient λ and the extinction coefficients of the clumped shortgrass canopies ($k_{\mathrm{NR}}(\theta)$) from the $T(\theta)$ measurements obtained with an LAI-2000 (in the denomination k_{NR}, the subscripts NR stands for non-random).

2.2. Using an LAI-2000 optical sensor for estimating extinction coefficients, PAR interception and PAR absorption in shortgrass canopies

2.2.1. The LAI-2000 optical sensor

The Li-Cor, LAI-2000 [1] is a hand-held instrument, whose optical sensor includes a fisheye lens and five silicon detectors allowing simultaneous measurements of the radiation coming from the upward hemisphere in five zenithal angles (Li-Cor, 1990; Welles and Norman, 1991). Silicon detectors respond approximately from 320 to 490 nm, in an area of the spectrum where leaf transmittance and reflectance are known to be low. Canopy transmittance in the five zenithal angles, $T(\theta)$, is estimated from measurements successively performed above and below the canopy. From these measurements, inversion of radiative transfer models allows the computation of PAI and MTA (Welles and Norman, 1991). Unlike $T(\theta)$, which is directly computed from radiation measurements, PAI and MTA result from model inversion. Their accuracy is therefore dependent on the degree to which model assumptions match reality. One of the main assumptions (that foliage elements are randomly distributed) departs significantly from reality in the case of clumped canopies where PAI estimations by LAI-2000 have been reported to underestimate PAI (e.g. Chason

[1] The use of company and brand names are necessary to report factually on available; however, the USDA neither guarantees nor warrants the standards of the products, and the use of the name by USDA implies no approval of the product to the exclusion of others that may also be suitable.

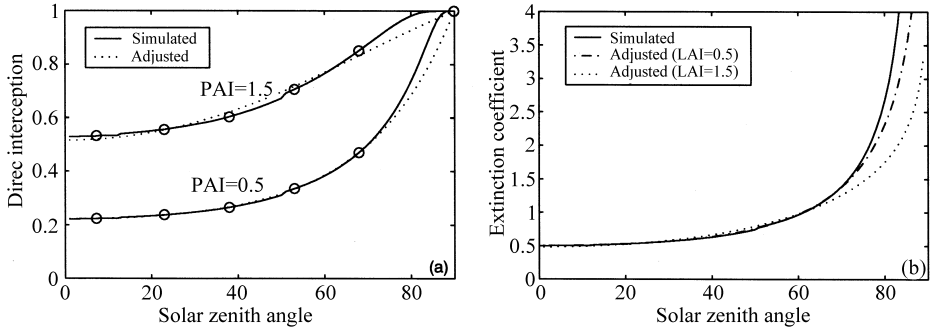

Fig. 1. Comparison between f_{direct} (a) or k (b) simulated (following Eqs. (3)–(7)) for the five LAI-2000 angles (○) and for all solar zenith angles (continuous lines) assuming an RLD, a spherical LAD and two PAIs (0.5 and 1.5) with f_{direct} (a) or k (b) adjusted following Hanan and Bégué (1995) (dashed lines) using Eq. (11) and the values of f_{direct} simulated in the five LAI-2000 angles.

et al., 1991; Chen et al., 1991; Fassnacht et al., 1994; Hanan and Bégué, 1995; Stenberg, 1996). However, even in the case of clumped canopies, if PAI is directly estimated with an appropriate methodology (e.g. with an LAI-3000 [2]) — or if the underestimation by LAI-2000 is quantified — the dependence of interception on solar zenith angle and PAI can be investigated.

2.2.2. Using LAI-2000 measurements and curve-fitting for estimating instantaneous and daily integrated PAR interception and absorption

LAI-2000 estimates $T(\theta)$ only in five zenith angles. However, Hanan and Bégué (1995) showed that these measurements provide enough information on the angular dependence of light interception for it to be interpreted for all solar zenith angles. In their approach, direct interception efficiency (the complement of $T(\theta)$) was estimated for all solar zenith angles by curve-fitting using the five interception efficiency values, and an additional point corresponding to the solar zenith angle 90°, for which interception efficiency tends to 1. The best-fit was of the form

$$f_{direct}(\theta) = \exp[a\cos(\theta) + b(\cos(\theta))^2], \quad (11)$$

where a and b are fitted coefficients. This simple equation was found to correctly fit the measured directional interception efficiency values, and PAR interceptions simulated from Eq. (2) (where $f_{diffuse}$ and $f_{direct}(\theta)$are successively computed from Eqs. (8) and (11)) were found to be in close agreement with measurements performed at 10 min intervals throughout the day. However, this simple equation may not fit well for any canopy structure, and a major drawback of this equation is that the coefficients a and b are dependent on the PAI for which they have been obtained; consequently, their estimated value cannot be used for estimating interception for different PAIs, therefore limiting the significance of the results. For this reason, it seems much more useful to have a methodology allowing the extrapolation of extinction coefficients $k(\theta)$ for all solar zenith angles, since coefficients $k(\theta)$ can be used to compute interception for different PAIs (Eq. (7)). The fitting process, however, may be much more cumbersome, as unlike for interception, the extinction coefficient tends to an infinite value for solar zenith angle tending to 90°.

It can be observed that Eq. (11) combined with Eq. (7) allows a formulation of $k(\theta)$ for all solar zenith angles:

$$k(\theta) = \frac{-c\ln\{1 - \exp[a\cos(\theta) + b(\cos(\theta))^2]\}}{(1 - \tau_f)}, \quad (12)$$

where c is the inverse of the PAI for which the values of the coefficient a and b have been estimated. However, as shown in Fig. 1, this simple formulation may not be appropriate for realistically simulating $k(\theta)$ for all solar zenith angles. In this figure, we assume a canopy with an RLD and a spherical distribution (calculated following De Wit (1965)), and direct interceptions are computed (from Eqs. (3)–(7)) for all solar zenith angles including the five LAI-2000 measurement angles, and for two different PAIs (0.5 and 1.5).

[2] Refer Footnote 1.

The directional interceptions in the five LAI-2000 angles and the point [90°; 1] are subsequently used for the curve-fitting as previously described. Fitted curves are compared to simulated ones in Fig. 1a, while Fig. 1b shows the comparison between the extinction coefficients estimated from Eq. (12) with the two sets of coefficients *a*, *b* and *c*, and the simulated extinction coefficients (Eq. (3)). The results show that in this case, for large solar zenith angles (>70°), Eq. (11) underestimates interception, and Eq. (12) underestimates the extinction coefficients. Furthermore, the underestimation of the extinction coefficient depends on the PAI for which the coefficients *a* and *b* have been obtained.

2.2.3. Using LAI-2000 measurements and the Markov model for estimating instantaneous and daily integrated PAR interception and absorption

Due to the limitations of the methodology presented above, our estimation of direct interception will not rely on it, but on the Markov model proposed by Nilson (1971) for canopies with non-random leaf dispersion. From this model, the canopy transmittance can be expressed as

$$T(\theta) = \exp[-\lambda(\theta)k(\theta)(1-\tau_f)\mathrm{PAI}], \quad (13)$$

where $\lambda(\theta)$ is a parameter accounting for non-random leaf dispersion; the product $\lambda(\theta)k(\theta)$ is the extinction coefficient of the heterogeneous canopy, $k_{NR}(\theta)$. Eq. (13), can therefore, be rewritten as

$$T(\theta) = \exp[-k_{NR}(\theta)(1-\tau_f)\mathrm{PAI}]. \quad (14)$$

The parameter λ is called 'Markov parameter' by several authors (e.g. Kuusk, 1995; Baldocchi and Collineau, 1994; Andrieu et al., 1997), or 'clumping index' (e.g. Chen and Black, 1991; Lacaze and Roujean, 1997), or 'leaf dispersion parameter' (e.g. Andrieu and Sinoquet, 1993; Baret et al., 1993). The term 'leaf dispersion parameter' will be used in this study. λ is greater than 1 when the leaves are regularly dispersed, equals 1 if leaves are randomly dispersed, and is less than 1 in the case of a clumped leaf dispersion; its value decreases as the clumpiness of the canopy increases. Although Nilson (1971) warned that in the same stand λ may vary with solar angle, and that such variations have been shown by several studies (e.g. Ross, 1975; Prévot, 1985; Andrieu and Sinoquet, 1993; Baret et al., 1993; Andrieu et al., 1997). In most studies, λ is assumed constant with respect to solar angle (e.g. Neumann et al., 1989; Qin, 1993; Qin and Jupp, 1993; Roujean, 1996). To our knowledge, with the exception of the pioneering work of Kuusk (1995), no deterministic method has yet been found for computing $\lambda(\theta)$ from canopy structure measurements, but it can be obtained empirically from comparison of measured and simulated gap fractions (e.g. Sinclair and Lemon, 1974; Sinclair and Knoerr, 1982; Neumann et al., 1989; Myneni et al., 1989; Baret et al., 1993; Andrieu et al., 1997; Chen et al., 1997). Gap fractions measured by the LAI-2000 may be useful for this purpose: if the LAD is measured, $k(\theta)$ can be computed for the five LAI-2000 measurements angles, and if PAI is estimated with an appropriate methodology, $k_{NR}(\theta)$ can be estimated from LAI-2000 gap fraction measurements (Eq. (14)). The directional leaf dispersion parameter, $\lambda(\theta)$, could therefore be estimated as

$$\lambda(\theta) = \frac{k_{NR}(\theta)}{k(\theta)}. \quad (15)$$

From the five estimated values of $\lambda(\theta)$, curve-fitting may be used to derive λ for other solar zenith angles. The extinction coefficients of the clumped canopy, $k_{NR}(\theta)$ and the gap fractions, $T(\theta)$ could therefore be computed for all solar zenith angles (Eqs. (13) and (14)), allowing the calculation of the efficiencies for direct and diffuse interception (Eqs. (7) and (8)), for instantaneous total interception and absorption (Eqs. (2) and (9)), and for daily interception and absorption (Eq. (10)).

3. Experiment

The experiment was carried out in 1996 as part of the semi-arid land-surface-atmosphere (SALSA) program, on different sites located in the Mexican part of the Upper San Pedro River Basin. This Basin was selected as the focal area for SALSA experiments (Goodrich et al., 1998), and spans the Mexico–US border from Sonora to Arizona. Several major vegetation types are represented in the basin, including riparian communities, desert shrub-steppe, grasslands, oak savanna and ponderosa pine woodlands.

Grasslands are dominated by C4 perennial bunchgrasses, which make up different communities according to topographic and edaphic conditions. Our study is focused on the plains grassland community in the Mexican part of the basin, found on the upland flats, gentle slopes and some lowlands, and dominated by shortgrasses and midgrasses, whose dominant species are grama species (*Bouteloua gracilis*, *B. repens*, *B. hirsuta*, *B. eriopoda*, *B. curtipendula*), three-awns (e.g. *Aristida ternipes*), lovegrasses (e.g. *Eragrostis intermedia*), and curly mesquite (*Hilaria belangeri*).

The annual precipitation ranges from 250 to 500 mm with approximately two-thirds falling during the 'monsoon season' from July to September (Osborn et al., 1972). This bimodal rainfall pattern promotes two growing periods, a minor one in late winter and early spring if temperatures are favorable, and the major one making up about 90% of the annual aboveground biomass production, during the summer monsoon season (Cable, 1975).

The experiment was carried out during the first 2 weeks of September 1996, close to the period of grassland peak biomass (Nouvellon, 1999). One site representative of the shortgrass prairie and located close to the village of Morelos was selected for heavy field measurements. On that site, species composition was quantitatively estimated, and some important canopy parameters such as clump densities, leaf-, stem- and plant-specific area (LSA, SSA and PSA), stems and leaf angle distribution (SAD and LAD), and plant area distribution as a function of the plant height were estimated all over the season for the main species. A more detailed description of these measurements is given in Nouvellon (1999). At the period of the measurements, the mean plant canopy height (defined as the height which includes 80% of the aboveground plant area) was 17.5 cm.

Gap fractions and radiation extinction coefficients in the five LAI-2000 measurement angles were estimated as follows:

First, PAI was estimated on 160 one m^2 plots in the experimental site. The plots were spaced every 10 m on 200 m transects oriented along the slight slope (about 1–2%). On each plot, PAI was estimated with the LAI-2000 from one reading above the canopy followed by five readings beneath the canopy, and another reading above the canopy. Inside the 1 m^2 plots, the five readings were taken systematically and evenly spaced along the diagonals (like the five dots on a die). According to the practical recommendations suggested by Li-Cor (1990), measurements were performed early in the morning, when the proportion of diffuse radiation was high, and the canopy around the sensor was shaded from direct solar radiation by placing the operator between the sensor and the solar location. A 180° view cap was used for obscuring the operator. After PAI was estimated with LAI-2000, on the same day, aboveground biomass on each plot was estimated from clipping plants, and weighing them after a 72 h drying period at 70°C. PAI was estimated on each plot from biomass measurements (g DM m^{-2}) and PSA (m^2 (g DM)$^{-1}$) obtained the same week for the main species.

In a second step, in order to increase the size of the sampling used for gap fraction estimations, gap fractions and PAI were estimated with LAI-2000 in 24 other shortgrass prairie sites distributed across the basin, and covering a wide range of PAI, due to varying soil conditions and grazing history. For each site, mean PAI and mean gap fractions on the five LAI-2000 measurement angles have been obtained from LAI-2000 measurements performed on 15 locations spaced every 15 m along transects, with the same protocol as the one described above.

4. Results

4.1. Destructive vs. non-destructive measurements

PAI estimated for the 160 plots using the LAI-2000 were compared to the PAI estimated from biomass and PSA estimations (Fig. 2). The results show the spatial variation of PAI along the transects and a good correlation between Li-Cor and PSA-estimated PAI values, despite a high scattering due to the small size of the plots. These results also indicate that LAI-2000 underestimates the PAI by about 12%. As previously mentioned, similar results have been obtained by several authors (e.g. Chason et al., 1991; Chen et al., 1991; Fassnacht et al., 1994; Hanan and Bégué, 1995; Stenberg, 1996). With the relationship presented in Fig. 2, it was possible to correct the underestimation of PAI measured with the LAI-2000 at the other 24 shortgrass ecosystem sites.

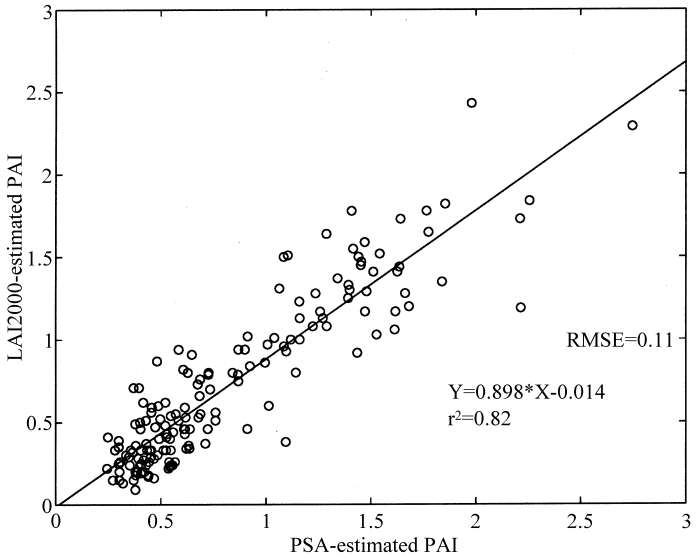

Fig. 2. Relationship between PAI estimated by LAI-2000 and PAI estimated from biomass and PSA measurements (Morelos site).

4.2. Canopy leaf and stem angle distributions

The orientation of foliage elements (e.g. stem and leaves) of the canopy is important information for describing light penetration in the canopy (e.g. Eq. (4)). LAD and SAD were estimated at the experimental site during the first week of September, taking into account the LAD and SAD of the main species, and their relative contribution to total leaf area and total stem area (Fig. 3a). The leaf and stem angle distribution (LSAD), the information required for describing light interaction within the canopy, was estimated from LAD and SAD and the relative contribution of leaves and stem to the total plant area.

SAD was found to be highly erectophile, while LAD was intermediate between a spherical and uniform distribution as described by De Wit (1965). In our study, we found that LAD changed significantly during the growing season (data shown in Nouvellon, 1999). Early in the season, LAD was found to be highly erectophile, and a progressive shift toward less erectophile LAD was observed along the growing season. Similar results have been reported for different perennial grass species (e.g. De Wit, 1965). However,

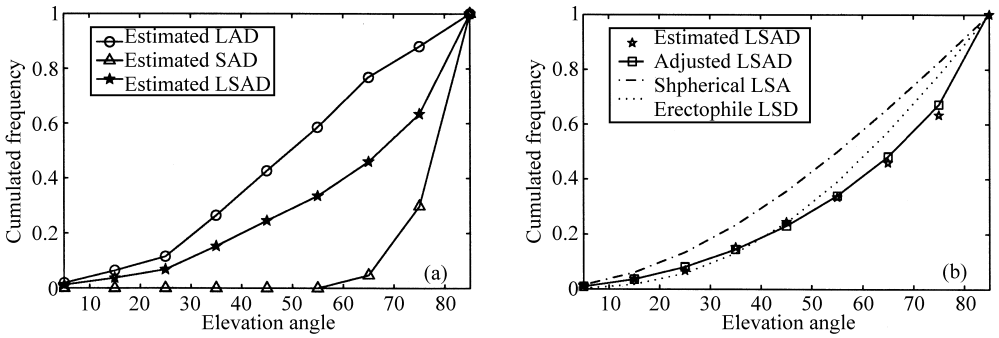

Fig. 3. LAD, SAD and LSAD estimated from measurements at the Morelos site (a), and comparison between estimated LSAD and LSAD adjusted using the two-parameter beta distribution function (b). An erectophile and a spherical LAD are presented for comparison.

the variations of LSAD over the season were less important than expected because the shift toward less erectophile LAD was compensated by a higher contribution of the highly erectophile stems to the total plant area in the later stages of plant development. A detailed description of seasonal changes in LSAD was not the focus of this study, and detailed information for these grasslands can be found in Bégué et al. (2000).

The computations performed further in this study required a mathematical expression for describing LSAD. To describe the LSAD, we therefore have used the two-parameter beta distribution function proposed by Goel and Strebel (1984):

$$g(\theta_l, \mu, \nu) = \frac{1}{\pi/2}\frac{\Gamma(\mu+\nu)}{\Gamma(\mu)\Gamma(\nu)}\left(1-\frac{\theta_l}{\pi/2}\right)^{\mu-1} \times \left(\frac{\theta_l}{\pi/2}\right)^{\nu-1}, \quad (16)$$

where θ_l represents the leaf (plus stem) inclination (here expressed in radian), μ and ν are the two parameters of the distribution, and $\Gamma(x)$ a gamma function which can be approximated by Goel and Strebel (1984):

$$\Gamma(x) \approx \left(\frac{2\pi}{x}\right)^{0.5} x^x e^y,$$
$$y = \frac{1}{12x} - \frac{1}{360x^3} - x. \quad (17)$$

The value of the two parameters μ and ν can be easily estimated from measured LSAD, as they only depend on the average and second moment of the leaf (plus stem) inclination angle, $\langle\theta_l\rangle$ and $\langle\theta_l^2\rangle$ (see Goel and Strebel (1984) for more details). Calculated $\langle\theta_l\rangle$ and $\langle\theta_l^2\rangle$ were 65.6 and 4739.7°, respectively (by comparison the mean MTA estimated from LAI-2000 measurements was 62.3°), and this resulted in μ and ν values of 0.7168 and 1.9242, respectively. From comparison of the cumulative inclination angles simulated using Eq. (16) with the measured cumulative inclination angles, one can observe the ability of the beta function to correctly reproduce the measured LSAD (Fig. 3b). Simulated LSAD was also compared with the LSAD of an erectophile and a spherical canopy (as defined by De Wit, 1965). This figure, as well as μ and ν values, indicates the pronounced erectophile characteristics of the canopy.

4.3. Directional radiation extinction coefficients $k(\theta)$

Fig. 4 shows gap fractions measured on the 25 sites in the five LAI-2000 angles plotted against the estimated PAI (corrected from the LAI-2000 underestimation, cf. Fig. 2). As expected, the canopy transmittance decreased as the PAI increased, and for all the five angles, Eq. (14) was found to fit very well the measured transmittances ($r^2 > 0.97$). The gap fractions decreased as the zenith angle increased, primarily because the path length of a ray of radiation inside the canopy increases with solar zenith angle (the path length is simply calculated as the height of the canopy divided by the cosine of zenith angle), and secondarily because for this LSAD, the fraction of foliage projected in the direction $\theta(G(\theta))$ increased with the zenith angle θ (Fig. 4f).

The clumping effect was evidenced by the fact that for each zenith angle the measured transmittances were significantly higher than the transmittances simulated for a canopy with an RLD and same LSAD (Fig. 4). The extinction coefficients $k_{NR}(\theta)$ obtained from the measurements for the five LAI-2000 angles are compared in Table 1 to the extinction coefficients $k(\theta)$ calculated for the RLD canopy.

The leaf dispersion coefficients $\lambda(\theta)$, calculated as the ratios between estimated extinction coefficients $k_{NR}(\theta)$ and simulated extinction coefficients $k(\theta)$, indicated that clumping effect was not negligible (Table 1, Fig. 5a). The reduction of the extinction coefficient in the clumped canopy was as high as 14% compared to the extinction coefficient of an RLD canopy. The clumping effect appeared to be poorly dependent of the solar zenith angle, as the dispersion parameter

Table 1
Extinction coefficients of the clumped shortgrass canopies $k_{NR}(\theta)$, estimated from LAI-2000 measurements, and extinction coefficients simulated for an RLD canopy with a same LSAD, $T(\theta)$

LAI-2000 angles, θ (°)	$k_{NR}(\theta)$	$k(\theta)$	$\lambda(\theta)$[a]
7.2	0.339	0.392	0.863
23	0.404	0.463	0.873
38	0.515	0.593	0.868
53	0.741	0.840	0.882
68	1.253	1.424	0.880

[a] The leaf dispersion parameter $\lambda(\theta)$ is calculated as the ratio between estimated $k_{NR}(\theta)$ and simulated $k(\theta)$.

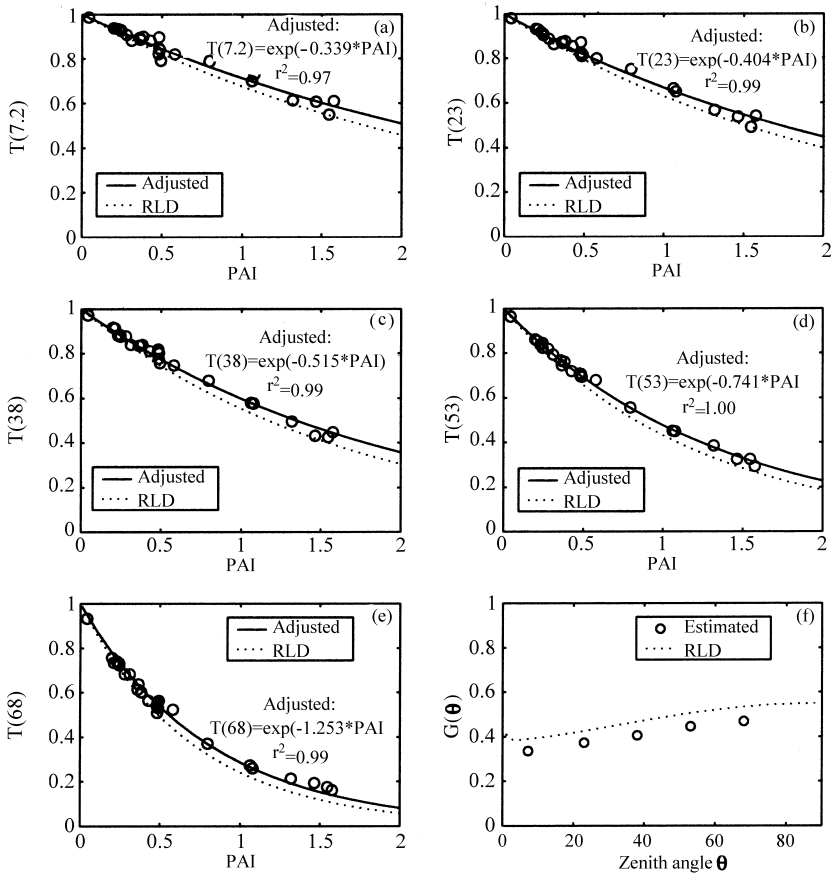

Fig. 4. Gap fractions $T(\theta)$ measured by LAI-2000 plotted against PAI (circles) (a–e). Continuous lines represent adjusted gap fractions. They are compared with gap fractions simulated for a canopy characterized by the same LSAD but with an RLD (dashed lines). (f) compares G values estimated from LAI-2000 gap fraction measurements (○) and G values simulated for the RLD canopy (dashed lines).

$\lambda(\theta)$ varied only in the range 0.86–0.88. However, we observed a very slight increase of $\lambda(\theta)$ with the solar zenith angles that was fitted with a linear equation (Fig. 5a). The latter equation was subsequently used to simulate the extinction coefficient of the clumped canopy for all solar zenith angles (Eq. (13)). The results showed a very good agreement between simulated extinction coefficients and extinction coefficients estimated for the five LAI-2000 measurement angles (Fig. 5b).

The method proposed for simulating the extinction coefficients of a clumped canopy for any solar zenith angle, using easily obtained LAI-2000 transmittance measurements might therefore be very useful due to its simplicity and accuracy. However, to obtain these results, we were required to use LSAD measurements which are time consuming to obtain and which are known to be approximate (Goel and Strebel, 1984; Kuusk, 1995; Andrieu et al., 1997). In order to test the sensitivity of the estimated extinction coefficient to the LSAD used for simulating them, we have applied the method using LSAD different from the measured LSAD. The results obtained using a spherical and a uniform LSAD distribution (as defined by De Wit, 1965) showed that estimated $\lambda(\theta)$ are highly sensitive to LSAD, so that slight errors on the estimation of LSAD would result in significant errors on $\lambda(\theta)$ estimations (Fig. 5c). On the other hand, the

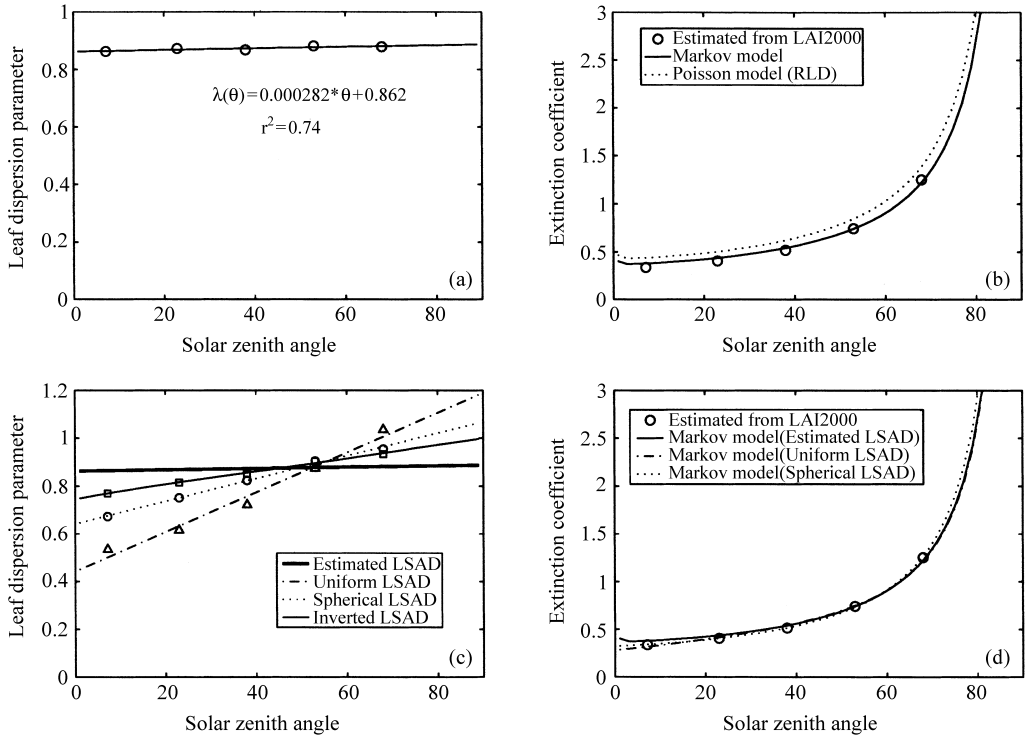

Fig. 5. Comparison of (a) the leaf dispersion parameters λ estimated from LAI-2000 gap fraction measurements and estimated LSAD (circles), and adjusted from the five estimated values of λ (continuous lines); (b) the extinction coefficients simulated from the Markov model using fitted values of λ (continuous lines), estimated from LAI-2000 measurements (circles), and simulated from the Poisson model (assuming an RLD) (dashed lines); (c) the leaf dispersion parameters λ adjusted from LAI-2000 measurements assuming a uniform LSAD (dashed line) or a spherical LSAD (dotted line), adjusted by inverting both the LSAD (Eqs. (16) and (17)) and Kuusk's model describing the angular course of λ (Eq. (18); continuous line), and adjusted using estimated LSAD (continuous bold line); (d) the extinction coefficients simulated from the Markov model using the values of λ estimated assuming a uniform LSAD (dashed line), a spherical LSAD (dashed line), and estimated LSAD (continuous lines).

extinction coefficients obtained using the spherical and a uniform LSAD were nearly indistinguishable from those obtained using the measured LSAD, and agreed very well with the extinction coefficients estimated for the five LAI-2000 measurement angles (Fig. 5d). These results are interesting as they suggest (1) that the inescapable errors associated with LSAD estimations might not have significantly affected our estimations of the extinction coefficients for any solar zenith angle, and (2) the method might be applicable without an accurate a priori knowledge of the LSAD of the canopy.

Furthermore, due to the strong sensitivity of $\lambda(\theta)$ to the LSAD, if a model exists to describe the angular course of the leaf dispersion parameter, it might be possible to invert the LSAD by comparing the estimated values of $\lambda(\theta)$ with the simulated ones. Such a model has been proposed by Kuusk (1995) for clumpy sparse canopies. The model describes the angular course of λ by accounting for the correlation of leaf positions in both horizontal and vertical directions (see also Kuusk (1991) for more details). In this model, the leaf dispersion parameter has its minimum value in the vertical position (where the dependence of the positions of canopy elements in neighboring layers is the highest), and increases to one toward the horizon. This angular course is expressed as (Kuusk, 1995)

$$\lambda(\theta) = 1 - (1 - \lambda_z)\frac{1 - \exp[-a\tan(\theta)]}{a\tan(\theta)}, \qquad (18)$$

where λ_z is the dispersion parameter in the vertical direction ($\lambda_z = \lambda(0)$), and a is a parameter which depends on the mean chord length of the leaves (Kuusk, 1991) and the height of the canopy, but is generally obtained by fitting (Kuusk, 1995). The feasibility of using Eq. (18) for inverting the LSAD had been tested using a procedure which minimized the difference between $\lambda(\theta)$ simulated following Eq. (18), and estimated in the five LAI-2000 measurements angles following Eq. (15). The values of the four unknown parameters (λ_z, a, μ and ν) were simultaneously adjusted, using a minimization algorithm based on the simplex method (Nelder and Mead, 1965). The values of the adjusted parameters converged toward a unique solution after a few iterations: 0.7448, 1.6322, 0.6841 and 1.4817 for λ_z, a, μ and ν, respectively. Adjusted $\lambda(\theta)$ and LSAD are presented in Figs. 5c and 6, respectively. The adjusted LSAD were found to be slightly less erectophile than the measured one. In the experiment, the bending of the leaves had not been measured and had not been taken into account for LSAD estimations. As a consequence, the LSAD estimated from measurements might slightly overestimate the erectophile character of the canopy (overestimate the MTA). The adjusted LSAD may therefore be closer to reality than the estimated one. MTA calculated from adjusted LSAD was 60.9°, which was close to the mean MTA estimated from LAI-2000 measurements (62.3°).

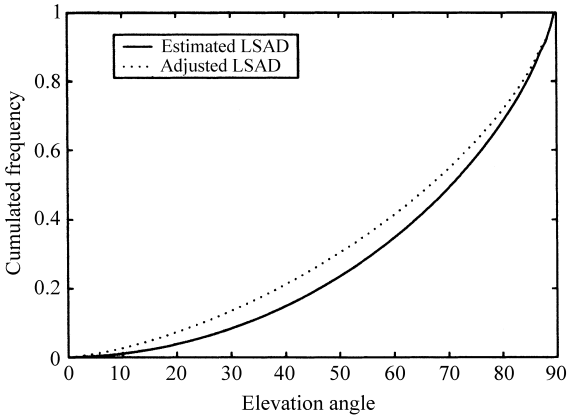

Fig. 6. Comparison of the LSAD adjusted by inverting the two-parameter beta distribution (together with Kuusk's model describing the angular course of λ) (dotted line), and the LSAD estimated from measurements (continuous line).

4.4. Instantaneous and daily integrated PAR interception and absorption

Unlike the extinction coefficients for direct solar radiation, total interception and absorption were not measured in our experiment. In the case of semi-arid grasslands sparse canopies, characterized by low PAI, previous studies (e.g. Bégué, 1991, 1992; Bégué et al., 1994; Hanan and Bégué, 1995) have already demonstrated that as soon as direct interception is correctly estimated (taking into account the clumping of the canopy), Eqs. (14), (8), (2) and (9) accurately reproduce the diurnal patterns of measured total interception and absorption. Our objective was not to present another validation of this model, but rather to assess some specific points that have been poorly documented for shortgrass prairies, namely (1) the effect of clumping, cloudy conditions and soil albedo on total absorption, and (2) the quantitative difference between IPAR and APAR.

The parameters required for the model are: (1) the incoming PAR geometry, (2) the optical properties of the leaves, and (3) the soil albedo in the PAR region. Concerning the PAR geometry, we have considered two cases: (1) a completely cloudy day for which the incoming PAR is totally diffused, and (2) a completely clear day. In the latter case, the proportion of diffuse radiation had been estimated following the empirical equation used by Bégué et al. (1994):

$$P_{\text{diffuse}}(t) = \frac{0.25}{0.25 + \cos(\theta_s)}. \tag{19}$$

Leaves reflectance, transmittance and absorptance in the PAR region had been estimated as 0.09, 0.04, and 0.87, respectively, from spectral data presented in Asner et al. (1998). Simulations were performed for two soil albedos: 0.15 and 0.25.

4.4.1. PAR interception

Efficiencies of direct, diffuse, and total hourly interception (f_{direct}, f_{diffuse} and f_{IPAR}, respectively) simulated for a completely clear day of the first week of September (DOY 246) for three contrasting PAI were compared with the efficiencies of an RLD canopy with the same LSAD (Fig. 7). For a completely cloudy day, f_{IPAR} equals f_{diffuse} and therefore exhibits no directionality, as shown from measurements by many studies

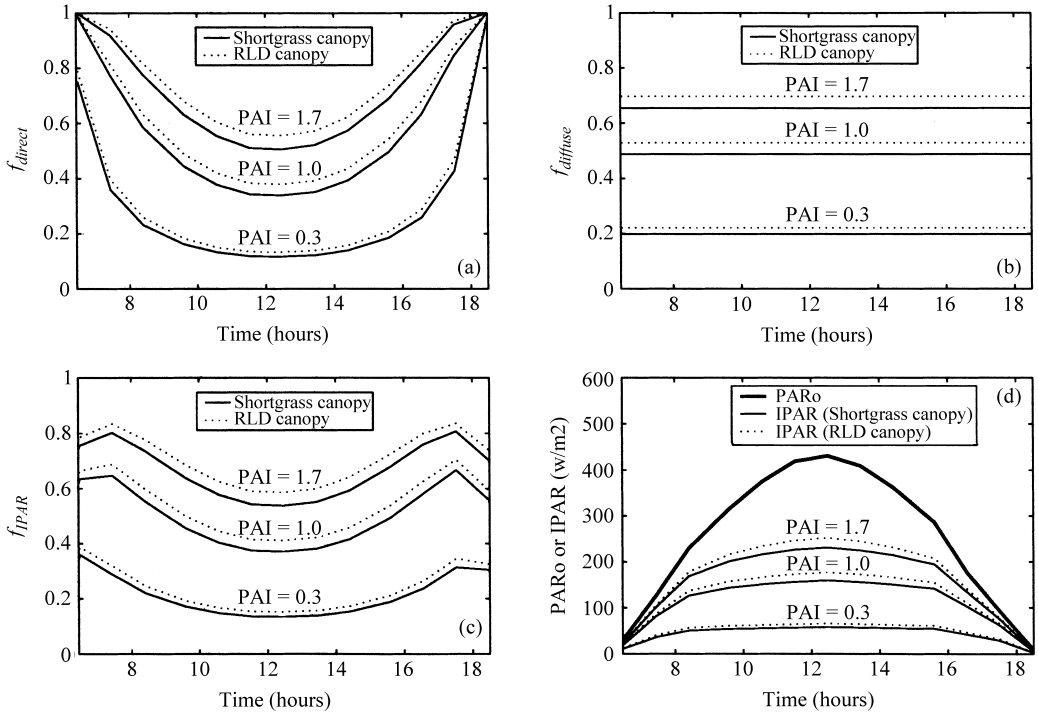

Fig. 7. Hourly interception efficiencies for direct radiation (a), for diffuse radiation (b), for total PAR (c), and fluxes of total PAR intercepted (d) simulated for a clear day (first week of September). The efficiencies estimated for the shortgrass canopies and for different PAIs (continuous lines) are compared to the efficiencies calculated for canopies with RLD (dotted lines).

(e.g. Impens and Lemeur, 1969; Hipps et al., 1983) for crop canopies. On the contrary, for a completely clear day, f_{IPAR} exhibited important directional effects. The 'dish shape' obtained is similar to those observed by Ripley and Redmann (1976) on a North-American mixed-grassland, or by Hanan and Bégué (1995) on a Sahelian grassland. For small solar angles, f_{diffuse} was higher than f_{direct} while for large solar angles, f_{diffuse} was lower than f_{direct}. This explained the decrease of total interception efficiencies for the largest solar angles associated with high proportions of diffuse radiation. The daily variations of PAR interception were much less than those of incoming PAR, as the interception efficiencies were the lowest when the incoming PAR was the highest (Fig. 7d).

The extinction coefficients for total interception $k_{\mathrm{IPAR}}(\theta)$ can be calculated from total interception estimations as

$$k_{\mathrm{IPAR}}(\theta) = \frac{-\ln[1 - f_{\mathrm{IPAR}}(\theta)]}{\mathrm{PAI}}. \quad (20)$$

The coefficients for a completely clear day and for a completely cloudy day are presented for two contrasted PAIs (Fig. 8). Unlike the extinction coefficients for direct solar radiation, the coefficients for diffuse

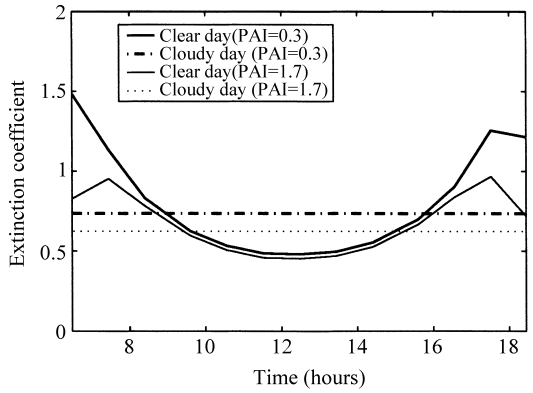

Fig. 8. Daily variations of the extinction coefficient of total PAR simulated for a clear day and a completely cloudy day, and for two contrasting PAIs.

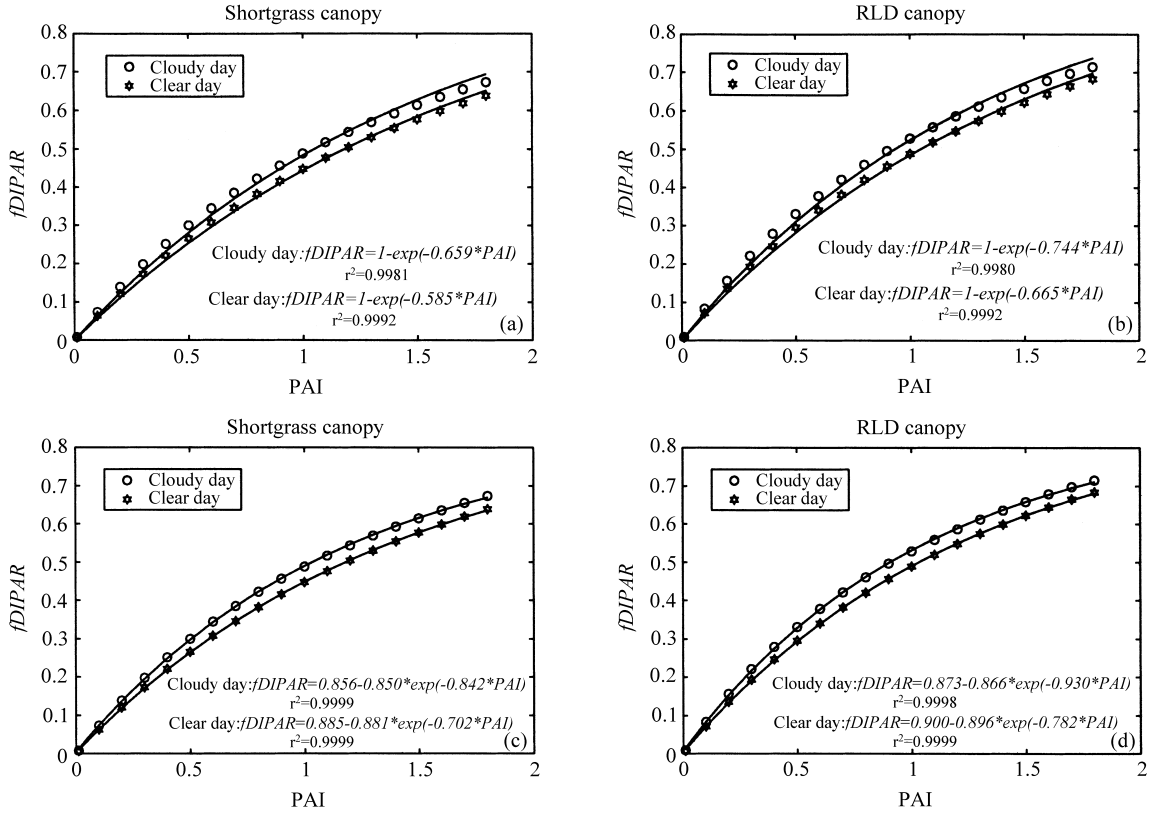

Fig. 9. Daily interception efficiencies of the shortgrass canopies (a and c) or the canopies with RLD (b and d), simulated for different PAIs, for a clear day (stars) and a completely cloudy day (circles). Continuous lines represent the curves adjusted from Eq. (1) (a and b) or from Eq. (21) (c and d). Adjusted equations are shown in each figure, and estimated coefficients are also reported in Table 2.

radiation, and consequently for total radiation, vary (decrease) with the PAI.

Daily interception efficiencies simulated for different PAIs were higher for a cloudy day than for a clear day (Fig. 9). The efficiencies for the RLD canopies were higher than for the clumped shortgrass canopies. The curves fitted using Eq. (1) appeared to underestimate f_{DIPAR} for low PAI, and to overestimate f_{DIPAR} for high PAI, especially for the cloudy day. This result is explained by the decrease of the extinction coefficients for diffuse and total radiation with PAI (Fig. 8). As a result, the relationship between f_{DIPAR} and PAI is better described by an equation with three parameters (Fig. 9c and d):

$$f_{\mathrm{DIPAR}} = a - b\exp(-k_2\,\mathrm{PAI}). \tag{21}$$

The fitted coefficients are reported in Table 2. For each case, coefficients a and b had very similar values. As a consequence, Eq. (21) can be simplified in an equation of two parameters:

$$f_{\mathrm{DIPAR}} = c[1 - \exp(-k_3\,\mathrm{PAI})]. \tag{22}$$

Low values of parameter c indicate that the curve departs importantly from the curve described by Eq. (1). For a day with a high proportion of diffuse radiation, c is expected to be lower than for a day with a low proportion of diffuse radiation. In Eqs. (21) and (22), parameters a and c represent the asymptotes of the curves (f_{DIPAR} for very high PAI), while the products bk_2 and ck_3 represent their initial slope. Comparisons of these coefficients indicate that the increase of f_{DIPAR} associated with higher ratio of diffuse:direct radiation is important for low PAI, while for very high values of PAI (which are not expected for such

Table 2
Estimated coefficients of the three exponential equations (Eqs. (1), (21) and (22)) used to describe the efficiencies of daily integrated interception (f_{DIPAR}) and absorption (f_{DAPAR}) in the shortgrass canopies or in RLD canopies, for a completely clear day or a completely cloudy day, and for two soil albedos

f_{DIPAR} or f_{DAPAR}	Day	Soil albedo	$Y = 1 - \exp(-k_1 \text{PAI})$		$Y = a - b\exp(-k_2 \text{PAI})$					$Y = c(1 - \exp(-k_3 \text{PAI}))$			
			k_1	r^2	a	b	k_2	bk_2	r^2	c	k_3	ck_3	r^2
Shortgrass canopy													
f_{DIPAR}	Clear	–	0.585	0.9992	0.885	0.881	0.702	0.618	0.9999	0.875	0.718	0.628	0.9999
f_{DIPAR}	Cloudy	–	0.659	0.9981	0.856	0.850	0.842	0.716	0.9999	0.845	0.869	0.734	0.9998
f_{DAPAR}	Clear	0.15	0.568	0.9963	0.784	0.779	0.828	0.645	0.9999	0.774	0.854	0.661	0.9999
f_{DAPAR}	Clear	0.25	0.611	0.9953	0.781	0.775	0.908	0.704	0.9998	0.771	0.937	0.722	0.9998
f_{DAPAR}	Cloudy	0.15	0.627	0.9941	0.771	0.765	0.960	0.734	0.9998	0.762	0.992	0.756	0.9997
f_{DAPAR}	Cloudy	0.25	0.670	0.9931	0.774	0.767	1.034	0.793	0.9998	0.765	1.070	0.819	0.9997
RLD canopy													
f_{DIPAR}	Clear	–	0.665	0.9992	0.900	0.896	0.782	0.701	0.9999	0.890	0.802	0.714	0.9999
f_{DIPAR}	Cloudy	–	0.744	0.9980	0.873	0.866	0.930	0.805	0.9998	0.862	0.961	0.828	0.9998
f_{DAPAR}	Clear	0.15	0.637	0.9958	0.798	0.792	0.917	0.726	0.9998	0.788	0.948	0.747	0.9998
f_{DAPAR}	Clear	0.25	0.684	0.9946	0.795	0.788	1.006	0.793	0.9998	0.786	1.040	0.817	0.9997
f_{DAPAR}	Cloudy	0.15	0.701	0.9933	0.786	0.779	1.058	0.824	0.9997	0.777	1.096	0.852	0.9997
f_{DAPAR}	Cloudy	0.25	0.748	0.9921	0.788	0.780	1.140	0.889	0.9997	0.780	1.182	0.922	0.9996

ecosystems), f_{DIPAR} for a cloudy day might be slightly lower than for a clear day. The fitted coefficients also indicate that clumping effect is important for low PAI, but tends to be negligible for high values of PAI.

4.4.2. PAR absorption

Instantaneous absorption efficiencies for different PAIs and the two soil albedos were compared to interception efficiencies (Fig. 10). Results showed that for a clear day, instantaneous absorption efficiencies presented less directionality than interception. However, the directional effect remained important. For example, for a PAI of 0.3 and a soil albedo of 0.25, absorption efficiency was 0.35 at 7 h and 0.16 at noon. When PAI was high and soil albedo was low, absorption was less than interception all over the day. The opposite pattern was obtained when PAI was low and soil albedo was high. In most cases, absorption was lower than interception for large solar zenith angles, and higher than interception for small solar zenith angles.

Daily integrated absorption efficiencies calculated as a function of PAI were compared with interception efficiencies (Fig. 11). The variations of f_{DAPAR} with PAI were very well described by Eq. (21). As for f_{DIPAR}, fitted parameters a and b were very similar, and therefore Eq. (22) fit very well f_{DAPAR}. This latter equation is used by most studies to fit measured f_{DAPAR} (e.g. Hipps et al., 1983). The values of the parameter c were much lower than for interception (Table 2). This indicated that (1) the departure from Eq. (1) is higher for absorption than for interception, and (2) for high PAI absorption is less than interception.

Further analysis of parameter c and the product ck_3 indicates the following:

1. Absorption during cloudy days was higher than during clear days when PAI was low (Fig. 12a), while the asymptotic value for a cloudy day was slightly less than for a clear day. For a PAI close to zero, f_{DAPAR} for a cloudy day was about 1.17 the f_{DAPAR} for a clear day. This ratio was only 1.05 for a PAI of 1.5. The effect of the diffuse:direct ratio was slightly higher for the shortgrass clumped canopy than it would be for an RLD canopy.
2. The clumping effect was high for low PAI, but low for high PAI (Fig. 12b). For a clear day and a PAI close to zero, absorption of an RLD canopy was approximately 1.14 the absorption of a clumped shortgrass canopy, while it was only 1.07 for a PAI of 1.5. The clumping effect was slightly higher for a clear day than for a cloudy day.
3. Higher soil albedo led to higher absorption for low PAI, but for high PAI the effect of soil albedo was negligible (Fig. 12c). The effect of soil albedo was

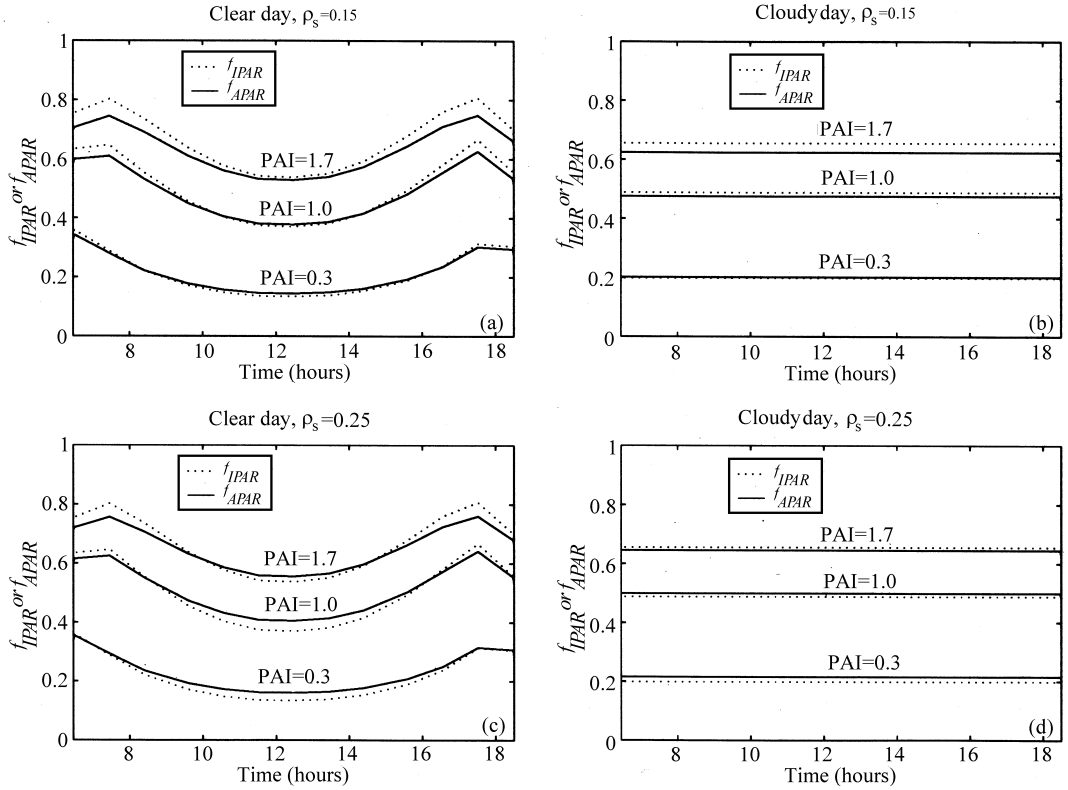

Fig. 10. Comparison of hourly absorption efficiencies (continuous lines) simulated for three PAIs, and hourly interception efficiencies (dotted lines). The efficiencies were calculated for a completely clear day (a and c) and a completely cloudy day (b and d), and for a soil albedo of 0.15 (a and b) or 0.25 (c and d).

slightly higher for a clear day than for a cloudy day (Fig. 12d).

4.4.3. Daily integrated absorption vs. daily integrated interception

Daily interception and absorption efficiencies for different PAIs, soil albedo and cloud conditions were compared (Fig. 13). For a soil albedo of 0.15, f_{DAPAR} was higher than f_{DIPAR} when the PAI was less than 0.5 (cloudy day) or 0.8 (clear day). When the PAI was higher than these thresholds, f_{DIPAR} was higher than f_{DAPAR}. The difference was not negligible (e.g. $f_{\mathrm{DIPAR}} = 1.04 f_{\mathrm{DAPAR}}$ for a PAI of 1.5). For a soil albedo of 0.25, f_{DAPAR} was higher than f_{DIPAR} until PAI as high as 1.4 (cloudy day) or 1.7 (clear day). For higher PAI, f_{DIPAR} was higher than f_{DAPAR}. The difference between f_{DAPAR} and f_{DIPAR} can be very significant for low PAI and high soil albedo. For example, for a soil albedo of 0.25 and a PAI close to zero, f_{DIPAR} was only 0.85 f_{DAPAR} (clear day).

5. Discussion and conclusions

Our objectives were to estimate the PAR extinction coefficients in shortgrass ecosystems, to study the effects of clumping, sky conditions, and soil albedo on PAR absorption, and to evaluate the difference between PAR interception and PAR absorption.

In a first step, gap fractions measured by an LAI-2000, together with independent measurements of PAI and LSAD, were used to estimate the leaf dispersion parameter $\lambda(\theta)$ of the Markov model. This parameter is a useful indicator of the clumpiness of the canopy and its estimation might therefore be a convenient way to track canopy structure changes

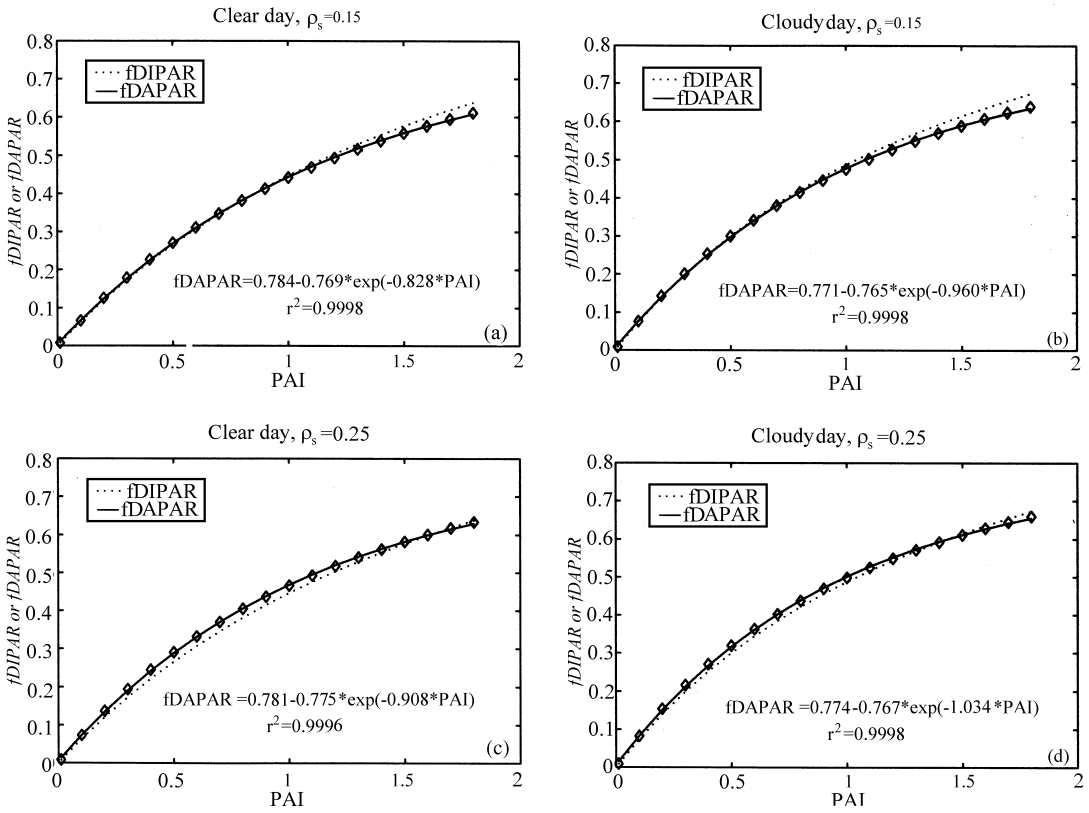

Fig. 11. Daily absorption efficiencies of the shortgrass canopies simulated for different PAIs (diamonds), for a completely clear day (a and c) or a completely cloudy day (b and d), and for a soil albedo of 0.15 (a and b) or 0.25 (c and d). Continuous lines represent the curves adjusted from Eq. (21). Adjusted equations are shown in each figure, and estimated coefficients are also reported in Table 2. Adjusted curves are compared to the curves adjusted to daily interception efficiencies (dotted lines).

associated with phenology, and to compare the clumping in canopies from different ecosystems.

Estimated $\lambda(\theta)$ were found to be highly sensitive to the LSAD used for their estimation. Similar results have been shown by Baret et al. (1993). This indicates that many estimates of $\lambda(\theta)$ reported in the literature may not be accurate, as they often have been obtained from approximate LSAD. Therefore, more attention should be paid to the accuracy of LSAD. Unfortunately, the methods currently used for measuring LSAD are time consuming and may not be very accurate (Goel and Strebel, 1984; Kuusk, 1995; Andrieu et al., 1997). On the other hand, thanks to the sensitivity of $\lambda(\theta)$ to LSAD, it has been shown that both the beta distribution describing LSAD and the Kuusk model describing the angular course of the leaf dispersion parameter $\lambda(\theta)$, can be simultaneously inverted using gap fractions measured with an LAI-2000.

In a subsequent step, extinction coefficients simulated for all solar zenith angles using Markov chain processes and estimated $\lambda(\theta)$ were used as input to a simple radiative transfer model taking into account first- and second-order scattering. Simulations of instantaneous and daily integrated PAR interception and absorption were subsequently used for studying the effects of clumping, sky conditions and soil albedo on PAR absorption.

Instantaneous PAR absorption showed marked directional effects for clear sky conditions. Consequently, for shortgrass ecosystems, the use of a constant extinction coefficient in canopy photosynthesis

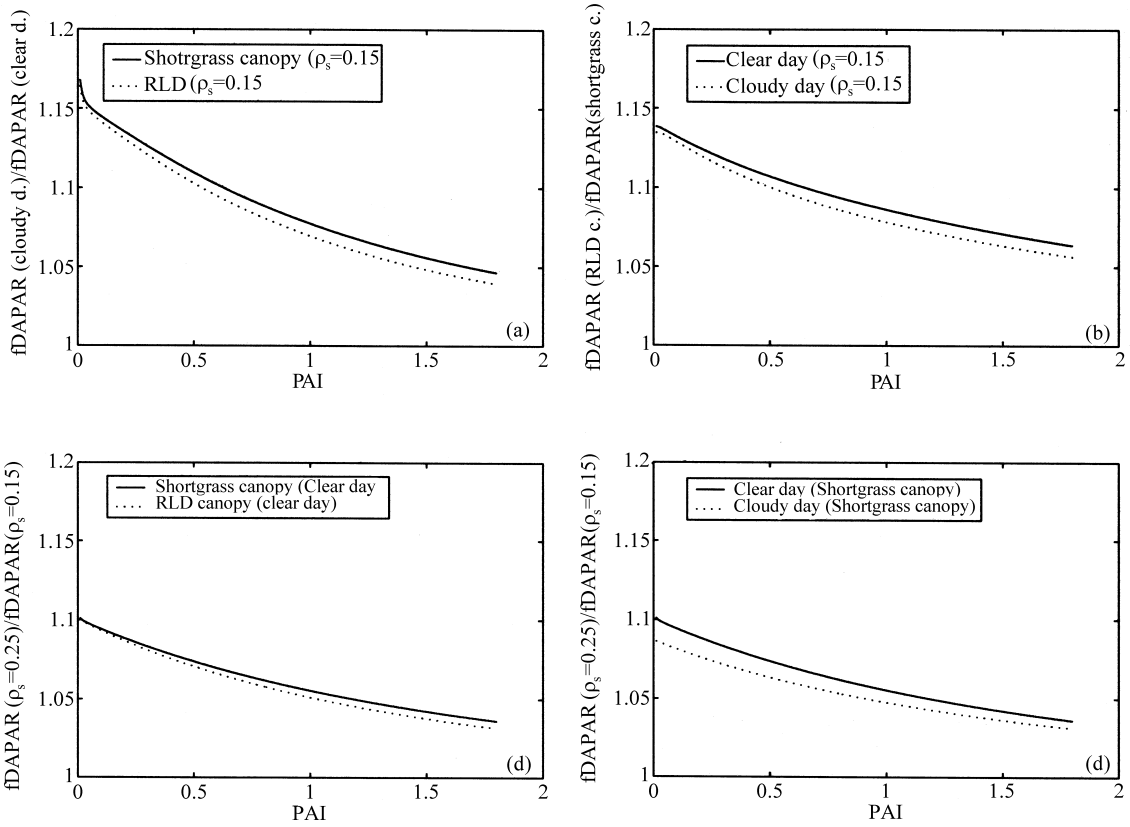

Fig. 12. Effects of sky conditions (a), clumping (b) and soil albedo (c and d) on the daily absorption efficiencies, as a function of PAI.

models working at an hourly time step would give inaccurate estimations of the PAR absorbed by the canopy.

The effects of clumping, sky conditions, and soil albedo were all found to be significant for low PAI, but much smaller for high PAI. These results are consistent with those of Hipps et al. (1983) who found that measured efficiencies of PAR absorption in wheat canopies were independent of sky conditions when PAI was high, but were significantly influenced by cloud clover when PAI was small. As shortgrass ecosystems are characterized by low PAI (e.g. Knight, 1973; Hazlett, 1992; Nouvellon, 1999), neglecting these effects would give inaccurate estimations of PAR absorption. To stress the importance of sky conditions, the increased absorption efficiencies for cloudy days coincide with higher climatic efficiencies (the proportion of PAR in the incoming solar radiation above the canopy) (Monteith, 1972; Bégué, 1991; Nouvellon, 1999). As both these effects are neglected in most canopy photosynthesis models, this might result in important underestimation of the PAR available for photosynthesis during cloudy days.

Daily PAR absorption was found to be significantly higher than PAR interception for low PAI, especially when soil albedo was high, and lower than PAR interception for high PAI. In canopy photosynthesis models, PAR absorbed by leaves is often estimated from simple exponential-like relationships calibrated using PAR interception measurements. Our results indicate that in such models, the PAR available for photosynthesis might be significantly underestimated in the first stages of the growth (when PAI is low), and may be overestimated in the later stages of the growing season.

In the present study, extinction coefficients derived from LAI-2000 measurements using a methodology

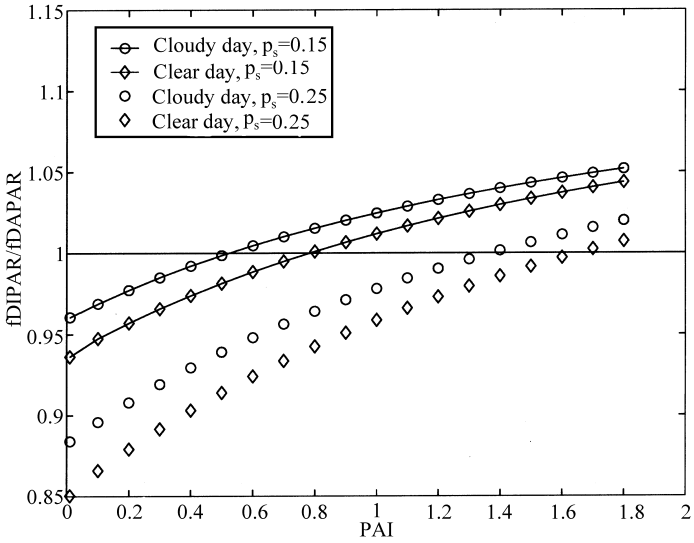

Fig. 13. Variations of the ratios between the daily interception efficiencies (f_{DIPAR}) and the daily absorption efficiencies (f_{DAPAR}) of the shortgrass canopies as a function of PAI. These ratios are presented for a clear day and for a cloudy day, and for two contrasting soil albedos.

based on Markov chain processes were incorporated in a simple radiative transfer model. They could instead be introduced in a more detailed multispectral radiative transfer model taking into account multiple scattering, hot spot, soil background bidirectional reflectance, etc. (Kuusk, 1995). It could satisfactorily simulate clumped canopy multispectral reflectance without the need for a heavy parameterization of canopy structure.

Acknowledgements

This research activity has been funded by Landsat 7 (NASA-S-1396-F) project and was carried out in the framework of SALSA-Global change research program (NASA grant W-18, 997), Monsoon'90 (IDP-88-086), and VEGETATION (58-5344-6-F806 95/CNES/0403). The CIRAD grant for Y. Nouvellon during his thesis research is gratefully acknowledged.

References

Anderson, M.C., 1966. Stand structure and light penetration. II. A theoretical analysis. J. Appl. Ecol. 3, 41–54.

Andrieu, B., Sinoquet, H., 1993. Evaluation of structure description requirements for predicting gap fraction of vegetation canopies. Agric. For. Meteorol. 65, 207–227.

Andrieu, B., Baret, F., Jacquemoud, S., Malthus, T., Steven, M., 1997. Evaluation of an improved version of SAIL model for simulating bidirectional reflectance of sugar beet canopies. Remote Sensing Environ. 60, 247–257.

Asner, G.P., Wessman, C.A., Archer, S., 1998. Scale dependence of absorption of photosynthetically active radiation in terrestrial ecosystems. Ecol. Appl. 8 (4), 1003–1021.

Baldocchi, D., Collineau, S., 1994. The physical nature of solar radiation in heterogeneous canopies: spatial and temporal attributes. In: Cadwell, M.M., Pearcy, R.W. (Eds.), Exploitation of Environmental Heterogeneity by Plants. Academic Press, San Diego, CA.

Baldocchi, D.D., Hutchison, B., Matt, D., McMillen, R.T., 1985. Canopy radiative transfer models for spherical and known leaf inclination angle distributions: a test in an oak–hickory forest. J. Appl. Ecol. 22, 539–555.

Baret, F., Andrieu, B., Steven, M., 1993. Gap fraction and canopy architecture of beet and wheat crops. Agric. For. Meteorol. 65, 261–279.

Bégué, A., 1991. Estimation de la production primaire en zone Sahélienne à partir de données radiométriques. Ph.D. Thesis. Université Paris VII, Paris.

Bégué, A., 1992. Modelling hemispherical and directional radiative fluxes in regular-clumped canopies. Remote Sensing Environ. 40, 219–230.

Bégué, A., Hanan, N.P., Prince, S.D., 1994. Radiative transfer in shrub savanna sites in Niger: preliminary results from HAPEX-Sahel. 2. Photosynthetically active radiation interception of the woody layer. Agric. For. Meteorol. 69, 246–266.

Bégué, A., Roujean, J.L., Hanan, N.P., Prince, S.D., Thawley, M., 1996a. Shortwave radiation budget of Sahelian vegetation. 1. Techniques of measurements and results during HAPEX-Sahel. Agric. For. Meteorol. 79, 79–96.

Bégué, A., Prince, S.D., Hanan, N.P., Roujean, J.L., 1996b. Shortwave radiation budget of Sahelian vegetation. 2. Radiative transfer models. Agric. For. Meteorol. 79, 97–112.

Bégué, A., Luquet, D., Dauzat, J., Nouvellon, Y., Rey, H., 2000. Architecture and radiation interception of a short-grass ecosystem: modeling approach using 3D computerized vegetation canopies, in preparation.

Cable, D.R., 1975. Influence of precipitation on perennial grass production in the semidesert southwest. Ecology 56, 981–986.

Campbell, G.S., 1986. Extinction coefficients for radiation in plant canopies calculated using an ellipsoidal inclination angle distribution. Agric. For. Meteorol. 36, 317–321.

Campbell, G.S., 1990. Derivation of an angle density function for canopies with ellipsoidal leaf angle distributions. Agric. For. Meteorol. 49, 173–176.

Chason, J.W., Baldocchi, D.D., Hutson, M.A., 1991. A comparison of direct and indirect methods for estimating forest canopy leaf area. Agric. For. Meteorol. 57, 107–128.

Chen, J.M., Black, T.A., 1991. Measuring leaf area index of plant canopies with branch architecture. Agric. For. Meteorol. 57, 1–12.

Chen, J.M., Black, T.A., Adams, R.S., 1991. Evaluation of hemispherical photography for determining plant area index and geometry of forest stand. Agric. For. Meteorol. 56, 129–143.

Chen, S.G., Shao, B.Y., Impens, I., Ceulemans, R., 1994. Effects of plant canopy structure on light interception and photosynthesis. J. Quant. Spectrosc. Radiat. Transfer 52 (1), 115–123.

Chen, J.M., Blanken, P.D., Black, T.A., Guilbeault, M., Chen, S., 1997. Radiation regime and canopy architecture in a boreal aspen forest. Agric. For. Meteorol. 86, 107–125.

Cowan, I.R., 1968. The interception and absorption of radiation in plant stands. J. Appl. Ecol. 5, 367–379.

De Wit, C.T., 1965. Photosynthesis of leaf canopies. Agriculture Research Report No. 663. Centre for Agriculture Publication and Documentation, Wageningen.

Fassnacht, K.S., Gower, S.T., Norman, J.M., McMurtrie, R.E., 1994. A comparison of optical and direct methods for estimating foliage surface area index in forests. Agric. For. Meteorol. 71, 183–207.

Gallo, K.P., Daughtry, C.S.T., Bauer, M.E., 1985. Spectral estimation of absorbed photosynthetically active radiation in corn canopies. Remote Sensing Environ. 17, 221–232.

Gastellu-Etchegorry, J.P., Demarez, V., Pinel, V., Zagolski, F., 1996. Modeling radiative transfer in heterogeneous 3D vegetation canopies. Remote Sensing Environ. 58, 131–156.

Goel, N.S., Strebel, D.E., 1984. Simple beta distribution representation of leaf orientation in vegetation canopies. Agron. J. 75, 800–802.

Goodrich, D.C., et al., 1998. An overview of the 1997 activities of the semi-arid land-surface-atmosphere (SALSA program). In: Proceedings of the 78th American Meteorological Society Annual Meeting, Phoenix, AZ, January 11–16, 1998.

Hanan, N.P., Bégué, A., 1995. A method to estimate instantaneous and daily intercepted photosynthetically active radiation using a hemispherical sensor. Agric. For. Meteorol. 74, 155–168.

Hazlett, D.L., 1992. Leaf area development of four plant communities in the Colorado steppe. Am. Midland Naturalist 127 (2), 276–289.

Hipps, L.E., Asrar, G., Kanemasu, E.T., 1983. Assessing the interception of photosynthetically active radiation in winter wheat. Agric. Meteorol. 28, 253–259.

Impens, I., Lemeur, R., 1969. Extinction of net radiation in different crop canopies. Arch. Met. Geophys. Biokl. Ser. B 17, 403–412.

Knight, D.H., 1973. Leaf area dynamics of shortgrass prairie in Colorado. Ecology 54, 891–896.

Kuusk, A., 1991. The hot spot effect in plant canopy reflectance. In: Myneni, R., Ross, J. (Eds.), Photon–Vegetation Interactions. Application in Optical Remote Sensing and Plant Ecology. Springer, New York, pp. 139–159.

Kuusk, A., 1995. A Markov chain model of canopy reflectance. Agric. For. Meteorol. 76, 221–236.

Lacaze, R., Roujean, J.L., 1997. Cartographie des paramètres de surface utiles au climat à partir des données multiangulaires POLDER pendant HAPEX-Sahel. In: Guyot, Phulpin (Eds.), Proceedings of the Seventh International Symposium on Physical Measurements and Signatures in Remote Sensing, Balkema, Rotterdam.

Lemeur, R., Blad, B.L., 1974. A critical review of light models for estimating the shortwave radiation regime of plant canopies. Agric. Meteorol. 14, 255–286.

Le Roux, X., Gauthier, H., Bégué, A., Sinoquet, H., 1997. Radiation absorption and use by humid savanna grassland: assessment using remote sensing and modelling. Agric. For. Meteorol. 85, 117–132.

Li-Cor, 1990. LAI-2000 plant canopy analyser operating manual. Li-Cor, Lincoln, NB.

Luquet, D., Bégué, A., Dauzat, J., Nouvellon, Y., Rey, H., 1998. Effect of the vegetation clumping on the BRDF of a semi-arid grassland: comparison of the SAIL model and ray tracing method applied to a 3D computerized vegetation. IGARSS'98, Seattle, WA, July 6–10, 1998.

Maas, S.J., 1988. Using satellite data to improve model estimates of crop yield. Agron. J. 80, 655–662.

Miller, J.B., 1967. A formula for average foliage density. Aust. J. Bot. 15, 141–144.

Monteith, J.L., 1969. Light interception and radiative exchange in crop stands. In: Eastin, J.D., Haskins, F.A., Sullivan, C.Y., van Bavel, C.H.M. (Eds.), Physiological Aspects of Crop Yield. American Society of Agronomy and Crop Science Society of America, Madison, WI, pp. 89–111.

Monteith, J.L., 1972. Solar radiation and productivity in tropical ecosystems. J. Appl. Ecol. 9, 747–766.

Myneni, R.B., Ross, J., Asrar, G., 1989. A review on the theory of photons transport in leaf canopies. Agric. For. Meteorol. 45, 1–153.

Nelder, J.A., Mead, R., 1965. A simplex method for function minimization. Comput. J. 7, 308–313.

Neumann, H.H., Den Hartog, G., Shaw, R.H., 1989. Leaf area measurements based on hemispheric photographs and leaf-litter

collection in a deciduous forest during autumn leaf-fall. Agric. For. Meteorol. 45, 325–345.
Nilson, T., 1971. A theoretical analysis of the frequency of gaps in plant stands. Agric. Meteorol. 8, 25–38.
Nouvellon, Y., 1999. Modélisation du fonctionnement de prairies semi-arides et assimilation de données radiométriques dans le modèle. Ph.D. Thesis. Institut National Agronomique Paris-Grignon.
Oker-Blom, P., Kellomaki, S., 1983. Effect of grouping of foliage on the with-stand and within-crown light regime: comparison of random and grouping canopy models. Agric. Meteorol. 28, 143–155.
Osborn, H.B., Lane, L.J., Hundley, J.F., 1972. Optimum gagging of thunderstorm rainfall in Southeastern America. Water Resour. Res. 8 (1), 259–265.
Prévot, L., 1985. Modélisation des échanges radiatifs au sein des couverts végétaux, application à la télédétection. Validation sur un couvert de mais. Ph.D. Thesis. Université Paris VI, 178 pp.
Qin, W.H., 1993. Modeling bidirectional reflectance of multi-component vegetation canopies. Remote Sensing Environ. 46, 235–245.
Qin, W.H., Jupp, D.L.B., 1993. An analytical and computationally efficient reflectance model for leaf canopies. Agric. For. Meteorol. 66, 31–64.
Ripley, E.A., Redmann, R.E., 1976. Grassland. In: Monteith, J.L. (Ed.), Vegetation and the Atmosphere. Vol. 2: Case Studies. Academic Press, London.
Ross, J., 1975. Radiative transfer in plant communities. In: Monteith, J.L. (Ed.), Vegetation and the Atmosphere, Vol. 1. Academic Press, London, pp. 13–52.
Ross, J., 1981. The radiation regime and architecture of plant stands. Junk, The Hague, Netherlands, 391 pp.
Roujean, J.L., 1996. A tractable physical model of shortwave radiation interception by vegetative canopies. J. Geophys. Res. 101 (D5), 9523–9532.
Saeki, T., 1963. Light relations in plant communities. In: Evans, L.T. (Ed.), Environmental Control of Plant Growth, Academic Press, New York, pp. 79–94.
Sheehy, J.E., Peacock, J.M., 1975. Canopy photosynthesis and crop growth rate of eight temperate forage grasses. J. Exp. Bot. 26 (94), 679–691.
Sinclair, T.M., Knoerr, E.R., 1982. Distribution of photosynthetically active radiation in the canopy of a doblolly pine plantation. J. Appl. Ecol. 19, 183–191.
Sinclair, T.M., Lemon, E.R., 1974. Penetration of photosynthetically active radiation in corn canopies. Agron. J. 66, 201–205.
Stenberg, P., 1996. Correcting LAI-2000 estimates for the clumping of needles in shoots of conifers. Agric. For. Meteorol. 79, 1–8.
van Gardingen, P.R., Jackson, G.E., Hernandez-Daumas, S., Russel, G., Sharp, L., 1999. Leaf area index estimates obtained for clumped canopies using hemispherical photography. Agric. For. Meteorol. 94, 243–257.
Verhoef, W., 1984. Light scattering by leaf layers with application to canopy reflectance modeling: the SAIL model. Remote Sensing Environ. 16, 125–141.
Warren Wilson, J., 1960. Inclined point quadrat. New Phytol. 58, 92–101.
Warren Wilson, J., 1963. Estimation of foliage denseness and foliage angle by inclined point quadrats. Aust. J. Bot. 11, 95–105.
Warren Wilson, J., 1965. Stand structure and light penetration. III. Analysis by point quadrats. J. Appl. Ecol. 2, 383–390.
Welles, J.M., Norman, J.M., 1991. Instrument for indirect measurement of canopy structure. Agron. J. 83 (5), 818–825.
Woledge, J., Parsons, A.J., 1986. Temperate grasslands. In: Backer, N.R., Long, S.P. (Eds.), Photosynthesis in contrasting environments. Elsevier, Amsterdam, pp. 173–197.